

Classification of interacting Dirac semimetals

Sheng-Jie Huang^{1,2,3}, Jiabin Yu,^{3,4} and Rui-Xing Zhang^{5,6,7,*}

¹Max Planck Institute for the Physics of Complex Systems, Nöthnitzer Str. 38, 01187 Dresden, Germany

²Joint Quantum Institute, Department of Physics, University of Maryland, College Park, Maryland 20742-4111, USA

³Condensed Matter Theory Center, Department of Physics, University of Maryland, College Park, Maryland 20742-4111, USA

⁴Department of Physics, Princeton University, Princeton, New Jersey 08544, USA

⁵Department of Physics and Astronomy, University of Tennessee, Knoxville, Tennessee 37996, USA

⁶Department of Materials Science and Engineering, University of Tennessee, Knoxville, Tennessee 37996, USA

⁷Institute for Advanced Materials and Manufacturing, University of Tennessee, Knoxville, Tennessee 37920, USA



(Received 4 June 2023; revised 23 May 2024; accepted 25 June 2024; published 11 July 2024)

Topological band theory predicts a \mathbb{Z} classification of three-dimensional (3D) Dirac semimetals (DSMs) at the single-particle level. Namely, an arbitrary number of identical bulk Dirac nodes will always remain locally stable and gapless in the single-particle band spectrum, as long as the protecting symmetry is preserved. In this work we find that this single-particle classification for C_n -symmetric DSMs will break down to $\mathbb{Z}_{n/\text{gcd}(2,n)}$ in the presence of symmetry-preserving electron interactions. Our theory is based on a dimensional reduction strategy which reduces a 3D Dirac fermions to one-dimensional building blocks, i.e., vortex-line modes, while respecting all the key symmetries. Using bosonization technique, we find that there exists a minimal number $N = n/\text{gcd}(2, n)$ such that the collection of vortex-line modes in N copies of DSMs can be symmetrically eliminated via four-fermion interactions. While this gapping mechanism does not have any free-fermion counterpart, it yields an intuitive “electron-trion coupling” picture. By developing a topological field theory for DSMs and further checking the anomaly-free condition, we independently arrive at the same classification results. Our theory paves the way for understanding topological crystalline semimetallic phases in the strongly correlated regime.

DOI: [10.1103/PhysRevB.110.035134](https://doi.org/10.1103/PhysRevB.110.035134)

I. INTRODUCTION

Semimetallic crystalline solids with vanishing density of states near the Fermi level usually carry nontrivial topological properties [1–4]. Dirac semimetal (DSM) is such an example with fourfold degenerate point nodes in the bulk energy band spectrum, whose nodal quasiparticles resemble massless Dirac fermions in three dimensions [5–12]. The Dirac points have symmetry-based \mathbb{Z} topological indices [11,12], and the manifestation of the topological indices lies in their exotic boundary modes (i.e., Fermi arc states). In particular, unlike doubly degenerate Weyl points, stabilizing the Dirac node (and the definition of the topological indices) in a three-dimensional (3D) crystal will necessarily require the crystalline symmetries. Thus far, experimental realizations of the DSM phase have been achieved in a plethora of quantum materials, including Na_3Bi , Cd_3As_2 , etc. [8,9], which have been attracting great research attention.

The ubiquitous electron correlations in quantum materials, however, could prevent band theory from faithfully describing real-world crystalline semimetals. For gapped topological

systems, it has been well established that interaction effects can enable a new topological phase that is free-fermion impossible, e.g., the anomalous surface topological orders in interacting topological insulators. Electron correlations can also trigger new topological equivalence relations between phases that are distinct in the noninteracting limit, qualitatively modifying the topological classification. Fidkowski and Kitaev first pointed out the $\mathbb{Z} \rightarrow \mathbb{Z}_8$ classification reduction for one-dimensional (1D) class BDI superconductors [13]. Similar reduction relations were later established for various crystalline topological insulators and superconductors [14–18]. Nonetheless, unlike their gapped cousins, little progress has been made towards understanding correlated gapless topological matters, where, in particular, their classification schemes have remained a fundamentally important open question. In this work, we uncover a $\mathbb{Z}_{n/\text{gcd}(2,n)}$ classification for C_n -symmetric correlated spinful DSMs by extending the frameworks of “topological crystals” [15,16,19–23] and crystalline gauge fields [24–32] to semimetallic phases. Compared with the \mathbb{Z} classification of free-fermion DSMs, this classification reduction is purely interaction driven. A key step of our framework is the successful dimensional reduction for DSMs, with which 3D Dirac fermions can be symmetrically “reduced” into 1D gapless fermionic vortex-line modes. This reduction procedure has been the main approach for classifying crystalline symmetry-protected topological phases [15,16,19,21]. As we apply it to DSMs, it well positions us to identify the lower-dimensional building blocks and to explore correlation effects of the residue 1D

*Contact author: ruixing@utk.edu

Published by the American Physical Society under the terms of the [Creative Commons Attribution 4.0 International](https://creativecommons.org/licenses/by/4.0/) license. Further distribution of this work must maintain attribution to the author(s) and the published article’s title, journal citation, and DOI. Open access publication funded by Max Planck Society.

vortex-line modes with the Luttinger liquid theory. In particular, we find that four-fermion interactions can gap out a collection of vortex-line modes without introducing any form of symmetry breaking if the vortex-line modes originate from $N = n/\text{gcd}(2, n)$ copies of identical DSMs. This concludes our classification for correlated DSMs, and the explicit gapping process can be understood through a *electron-trion coupling* picture. We further develop a topological field theory for DSMs and derive the $\mathbb{Z}_{n/\text{gcd}(2, n)}$ classification by checking the anomaly-free condition. Relations between our theory and the Lieb-Schultz-Mattis constraint are also discussed.

II. BAND THEORY OF DIRAC SEMIMETALS

In a 3D C_n -symmetric spinful crystal with both inversion symmetry \mathcal{P} and time-reversal symmetry (TRS) Θ , all energy bands must pair up to form degenerate band doublets. Along the C_n -invariant k_z axis, two bands constituting a doublet are labeled by their \hat{z} -component angular momenta $\{J, -J\}$ with J being an half-integer. When two doublets of bands cross at a generic $k_z = k_0$, they form a stable fourfold degenerate Dirac node, when they carry inequivalent angular momenta with $|J| \not\equiv |J'| \pmod{n}$. Assuming k_0 is not a time-reversal invariant momentum, TRS requires the presence of a partner Dirac node at $k_z = -k_0$ formed by the same set of bands, a manifestation of the fermion doubling theorem. The topological stability of a Dirac point is guaranteed by a \mathbb{Z} -type symmetry charge \mathcal{Q}_J [11,12]. Respecting the symmetries, a Dirac point can develop a gap only when merging with another oppositely charged Dirac point at the same momentum. Note that the key symmetries involved in the protection of a stable Dirac point are $U(1)$ charge conservation, C_n rotation, inversion-time-reversal $\mathcal{P}\Theta$, and a lattice translation along the rotation axis.

Without loss of generality, we assume all Dirac points in a C_n -symmetric DSM (denoted as DSM_n) sitting at $k_z = \pm k_0$, i.e., the two ‘‘valleys’’ labeled by an index $v = \pm$. The \hat{z} -directional lattice translation symmetry \mathcal{T}_z promotes the valley index v to be a good quantum number to mark the low-energy Dirac fermions. Meanwhile \mathcal{T}_z acts on the fermions as a valley $U(1)$ rotation $\exp(i\alpha_z\varphi)$, where the phase angle φ can be promoted to take continuous values at low energies. At each valley v , the minimal Hamiltonian for a single Dirac point reads

$$H_0^{(v)}(\mathbf{k}) = k_x\gamma_1 + k_y\gamma_2 + vk_z\gamma_5 + O(k^2), \quad (1)$$

where we have defined the γ matrices $\gamma_1 = \tau_3 \otimes \sigma_1$, $\gamma_2 = \tau_3 \otimes \sigma_2$, $\gamma_3 = \tau_1 \otimes \sigma_0$, $\gamma_4 = \tau_2 \otimes \sigma_0$, $\gamma_5 = \tau_3 \otimes \sigma_3$, and $\gamma_{jk} = \frac{1}{2i}[\gamma_j, \gamma_k]$, $\forall j < k$. Here k_z is an effective crystal momentum relative to the valley. The inversion symmetry and TRS are represented by $\mathcal{P} \doteq \alpha_x \otimes \gamma_5$ and $\Theta \doteq i\alpha_x \otimes \gamma_{13}\mathcal{K}$, respectively, where $\alpha_{x,y,z}$ are Pauli matrices for the valley degree of freedom (d.o.f.) and \mathcal{K} the complex conjugate [33]. Under this basis choice, C_n has a diagonal matrix representation $C_n \doteq \exp(i\frac{2\pi}{n}J)$, where $J = \text{diag}(l + \frac{1}{2}, l - \frac{1}{2}, -l + \frac{1}{2}, -l - \frac{1}{2})$ and $l < n/2$ is a positive integer. One can again check that a single-particle Dirac mass for Eq. (1) must break either C_n or \mathcal{T}_z [34].

Dimensional reduction

Although the gaplessness of free-fermion DSMs is symmetrically irremovable, we find it's possible to reduce the dimensionality of the gapless d.o.f. from three dimensions to one while respecting all the key symmetries. This *dimensional reduction* procedure for Dirac fermions is motivated by the observation that (γ_3, γ_4) forms a vector representation of C_n . We thus define $\gamma_{\pm} = \frac{1}{2}(\gamma_3 \pm i\gamma_4)$ and find that

$$C_n\gamma_{\pm}C_n^{-1} = e^{\pm i\frac{2\pi}{n}l}\gamma_{\pm}, \quad (2)$$

namely, γ_{\pm} carry angular momenta $J = \pm 2l$, respectively. As $\gamma_{3/4}$ breaks C_n explicitly, we need to couple γ_{\pm} to some spatial-dependent functions with proper angular momenta to preserve C_n . This motivates us to consider a vortex mass term for the Dirac point at valley v ,

$$H_v^{(v)}(r, \theta) = vm_0(r)[e^{iv\theta}\gamma_+ + e^{-iv\theta}\gamma_-], \quad (3)$$

where (r, θ) are the in-plane polar coordinates with $r = \sqrt{x^2 + y^2}$ and $\theta = \tan^{-1}(y/x)$. We choose $m_0(r) = m_0$ to be spatially uniform. To respect both C_n and $\mathcal{P}\Theta$, the vorticity ν of the vortex mass must satisfy

$$\nu = pn - 2l \quad (4)$$

with $\nu \in 2\mathbb{Z}$ and $p \in \mathbb{Z}$. Importantly, H_v is unable to eliminate all gapless d.o.f., as we analytically derived the gapless vortex-line modes dispersing along k_z in the presence of H_v . (See Appendix A for details.) The vortex-line modes are found to carry a half-integer-valued z -component angular momentum $J \pmod{n}$, with

$$\begin{aligned} l - \frac{1}{2} < J < \nu + l + \frac{1}{2}, & \quad \text{for } \nu > 0, \\ \nu + l - \frac{1}{2} < J < l + \frac{1}{2}, & \quad \text{for } \nu < 0. \end{aligned} \quad (5)$$

One can check that the number of zero modes is given by $|\nu| = |pn - 2l|$. Using perturbation theory, we find that the vortex-line mode at valley v is locally chiral with $E(k_z) = \text{sgn}(\nu v)k_z$ and an angular momentum label J . Due to this *chirality-valley locking* effect, in Appendix B we find it impossible to symmetrically gap out the $2|\nu|$ chiral modes in a ‘‘minimal’’ DSM_n with a pair of Dirac nodes, even when interaction effects are considered. This completes our dimensional reduction procedure, where we have successfully ‘‘reduced’’ 3D Dirac physics into 1D vortex-line modes in a fully symmetric manner. The vortex-line modes are thus the *1D building blocks* for general 3D DSMs, which is illustrated in Fig. 1 for DSM_3 .

III. CLASSIFICATION AND INTERACTION EFFECTS

Classifying DSM_n s is equivalent to studying the stability problem of Dirac points. Consider $N \in \mathbb{Z}_{>0}$ identical copies of minimal DSM_n s, each featuring a pair of Dirac nodes at $\pm k_0$. This DSM_n phase will admit a \mathbb{Z}_N classification, if there exists a minimal N such that all Dirac nodes can be gapped out thoroughly without introducing (i) explicit or spontaneous symmetry breaking or (ii) topological order. Otherwise, the DSM_n is \mathbb{Z} classified.

We now attack this classification problem with the help of dimensional reduction procedure. Take DSM_3 as an example,

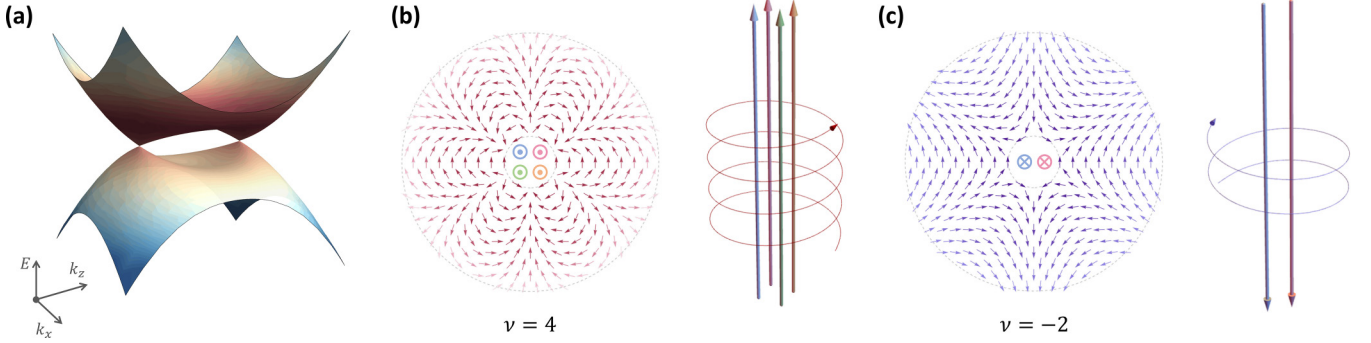


FIG. 1. Dimensional reduction of DSM. For a DSM_3 with a pair of Dirac points as shown in (a), the minimal vorticities for a vortex (antivortex) mass is $\nu = 4$ ($\nu = -2$), as shown in (b) and (c). The vortex will trap $|\nu|$ 1D gapless vortex-line modes at each valley for DSM_3 , whose propagating direction depends on $\text{sgn}(\nu)$. Only vortex modes at the $\nu = +$ valley are shown here.

where the basis index $l = 1$ is the only choice respecting $0 < l < n/2$. We define $\mathcal{V}_n = (\nu_v, \nu_{\text{av}})$ to denote the minimal symmetry-allowed vorticity for vortex ($\nu_v > 0$) and antivortex ($\nu_{\text{av}} < 0$) for DSM_n . Equation (4) immediately implies that $\mathcal{V}_3 = (4, -2)$, and a summary of \mathcal{V}_n can be found in Table I. We further denote $\psi_{v,J,R/L}$ as a fermion operator that annihilates a right/left chiral vortex-line mode with an angular momenta J at valley v . In particular, a $\nu = 4$ vortex harbors four right-moving vortex-line modes $\Psi_{+,v=4}^{(3)} = (\psi_{+,\frac{3}{2},R}, \psi_{+,\frac{1}{2},R}, \psi_{+,-\frac{1}{2},R}, \psi_{+,-\frac{3}{2},R})$, and a $\nu = -2$ antivortex traps two left movers $\Psi_{+,v=-2}^{(3)} = (\psi_{+,\frac{1}{2},L}, \psi_{+,-\frac{1}{2},L})$ at the $+k_0$ valley. The $-k_0$ valley states are TRS-related with $\Psi_{-,v}^{(3)} = \Psi_{+,v}^{(3)} (R \leftrightarrow L)$. At the free-fermion level, it is straightforward to check the inability to find a combination of vortices and antivortices that can gap out the vortex-line modes, a manifestation of the \mathbb{Z} classification of noninteracting DSMs.

When interaction effects are considered, the 1D vortex-line modes are readily described by the Luttinger liquid theory. Using the bosonization technique, we show that for DSM_n , a group of vortex-line modes can always be symmetrically gapped out if the net vorticity vanishes. (See Appendix B for details.) As a result, for $N = 3$ copies of DSM_3 , one can give one DSM_3 copy a $\nu = 4$ vortex and the other two with a $\nu = -2$ vortex each. Then the cancellation of vorticities directly implies the symmetry-preserving gapping of the vortex-line

TABLE I. Classifications of 3D Dirac semimetals with C_n rotation symmetries for $n = 3, 4, 6$. All DSM_n s admit a \mathbb{Z} classification for a fixed choice of symmetry representation (labeled by l in this paper) in the free-fermion limit except for $n = 2$, where the free fermion classification is already trivial [11]. In the second column, $\mathcal{V}_n = (\nu_v, \nu_{\text{av}})$ denotes the minimal vorticities for vortex and antivortex. The interacting classification for DSM_n is given by $\mathbb{Z}_{n/\text{gcd}(2,n)}$, as derived from the bosonization theory and the quantum anomaly analysis.

Rotation	Vorticity	Free-fermion	Interacting
$n = 3$	$(4, -2)$	\mathbb{Z}	\mathbb{Z}_3
$n = 4$	$(2, -2)$	\mathbb{Z}	\mathbb{Z}_2
$n = 6$	$(4, -2)$ or $(-4, 2)$	\mathbb{Z}	\mathbb{Z}_3

modes, immediately leading to a \mathbb{Z}_3 classification of DSM_3 . Namely, DSM_3 s with N pairs of Dirac points can be gapped out symmetrically by interactions, as long as N is an integer multiple of 3.

For DSM_4 , we have $\mathcal{V}_4 = (2, -2)$. Therefore, two identical copies of vortex-incorporated DSM_4 , one with a vortex and another with an antivortex, will enable a symmetric gapping, further leading to the \mathbb{Z}_2 classification for DSM_4 . For DSM_6 , there exist two different basis choices with $l = 1, 2$, which leads to $\mathcal{V}_6^{(l=1)} = (4, -2)$ and $\mathcal{V}_6^{(l=2)} = (2, -4)$, respectively. For both scenarios, we will need three copies of DSM_6 to realize the cancellation of vorticity, similar to the case in DSM_3 . We thus conclude that DSM_6 generally admits a \mathbb{Z}_3 classification in the correlated limit. A summary of classification of DSM_n in both free-fermion and interacting limits can be found in Table I.

A. Electron-trion coupling

We now provide an alternative yet intuitive ‘‘trion’’ picture to understand how a symmetric many-body gap will naturally arise in DSM_n . Let us focus on DSM_3 , where the low-energy vortex-line modes involved in a three-vortex configuration are one $\Psi_{+,v=4}^{(3)}$ and two $\Psi_{+,v=-2}^{(3)}$ at valley $+k_0$, as well as their TRS partners. We consider a four-fermion term

$$H_{\text{ET}} = \psi_{+,\frac{3}{2},R}^\dagger \Phi_{+,\frac{3}{2},L}, \quad (6)$$

where $\Phi_{+,\frac{3}{2},L} = \psi_{-,-\frac{1}{2},R}^\dagger \psi_{+,-\frac{1}{2},L} \psi_{-,\frac{3}{2},L}$ annihilates a left-moving three-particle excitation (i.e., a trion [35]). Clearly, the trion carries exactly the same set of symmetry indices as that of $\psi_{+,\frac{3}{2},R}^\dagger$, so that the above electron-trion interaction is symmetry-preserving and will unambiguously gap out the vortex mode generated by $\psi_{+,\frac{3}{2},R}^\dagger$.

When the net vorticity of vortex masses vanishes, the collection of vortex-line modes are nonchiral as a whole. This ensures that we can write a complete set of electron-trion terms to gap out all fermionic d.o.f., which is further supported by an explicit bosonization analysis in Appendix B. Since $\psi_{+,\frac{3}{2},L}$ is absent in the vortex-line mode basis, the trion $\Phi_{+,\frac{3}{2},L}$ does *not* have any single-fermion counterpart that share both the same symmetry labels and the chirality.

Therefore, the above gapping process is only possible via many-body interactions.

B. Topological field theory and quantum anomaly

Here we derive the classification from the effective field theory of the Dirac semimetal. A brief review of the crystalline gauge fields and the relation to spatially dependent mass terms is given in Appendix C (see also Refs. [24–32]). We couple the theory to the crystalline gauge fields through adding the spatially dependent mass terms such as the vortex mass discussed above, which is the approach introduced in Ref. [31].

To explicitly couple the 3D Dirac semimetal to a translation gauge field in the z direction, we add the following spatially dependent mass term [in addition to the vortex mass (3)]:

$$H_z = m' e^{i\kappa\phi(z)\gamma_5}, \quad (7)$$

where $\kappa = 2k_0/2\pi$, and $2k_0$ is the momentum separation of the Dirac points at the two valleys. Translation in the z direction acts on ϕ by shifting $\phi \rightarrow \phi + 2\pi\mathbb{Z}$.

After coupling the Dirac semimetal to a $U(1)$ gauge field in the presence of these spatially dependent mass terms and integrating out the Dirac fermions, we obtain the unquantized topological term:

$$S = \kappa \int A \wedge E_z \wedge d\omega^{(n)}, \quad (8)$$

where $E_z = d\phi/2\pi$ are the translation gauge field and $\omega^{(n)} = dn_\theta/2\pi$ with $n_\theta = \nu\theta$ is the rotational gauge field. Note that E_z and $\omega^{(n)}$ are in the nontrivial cohomology class in $H^1(B\Gamma, \mathbb{Z})$ and $H^1(BC_n, \mathbb{Z})$, respectively (see Appendix D for more details). For a single DSM, one can show that the 2-form $d\omega^{(n)}$ must satisfy

$$\int_{M_{xy}} d\omega^{(n)} = \nu \bmod n, \quad (9)$$

where M_{xy} is a xy plane. The topological term (8) is not gauge invariant since κ is fractional, which signals the quantum anomaly. If we integrate over the xy plane, we find the anomaly localized and there is a 1D filling anomaly [28] for the vortex-line modes.

Now we show how to derive the classification of the Dirac semimetals from the field theory perspective. When we have N copies of the Dirac semimetal, the 2-form $d\omega^{(n)}$ satisfies

$$\int_{M_{xy}} d\omega^{(n)} = N(\nu \bmod n) \bmod n = N\nu \bmod n. \quad (10)$$

When $\int d\omega^{(n)} = 0 \bmod n$, the rotation gauge field is in the trivial cohomology class and the anomaly in Eq. (8) vanishes, which implies that the Dirac semimetals can be gapped out while preserving the symmetry. Note that $\nu \in 2\mathbb{Z}$ due to \mathcal{PT} symmetry. Therefore, the classification can be obtained by solving the equation $N\nu = 0 \bmod n$. As elaborated in Appendix E, the solution to the equation is $N \in \frac{n}{\gcd(|\nu|, n)}\mathbb{Z}$. For these numbers of copies of the Dirac semimetals, the topological response term (8) actually vanishes. This implies that the Dirac semimetals are unstable and can be gapped

out by strong interactions. Hence, interacting classification of the Dirac semimetals is given by $\mathbb{Z}_{\frac{n}{\gcd(|\nu|, n)}}$ with the minimum allowed value of $|\nu| = 2$, which is consistent with the result obtained by the direct analysis of the dimension reduction summarized in Table I [36].

IV. DISCUSSION AND CONCLUSIONS

We have shown that correlated 3D spinful Dirac semimetals yield a qualitatively different $\mathbb{Z}_{\frac{n}{\gcd(|\nu|, n)}}$ classification from that of their free-fermion counterparts (i.e., \mathbb{Z}). Our classification theory is based on identifying the low-dimensional building blocks for DSMs by coupling the Dirac fermions to fully symmetric vortex masses. Remarkably, the 1D blocks are gapless vortex-line modes that are symmetrically irremovable at the free-fermion level. This dimensional reduction technique enables both an exact bosonization approach to deal with electron correlation effects and a topological field theory construction to analyze quantum anomaly of DSMs, both of which lead to the same classification result for interacting DSMs. We note that while our theory is physically reasonable, a mathematical rigorous proof of the classification is still an open question.

When there are $N < n/\gcd(2, n)$ copies of DSM_n , the system is a symmetry-protected correlated gapless phase. To generate mass for the Dirac fermions, one will then have to either break the symmetries [34] or introduce electron fractionalization [37,38]. In other words, for $N < n/\gcd(2, n)$, our classification suggests the absence of any symmetric featureless insulators, which manifests as a generalized Lieb-Schultz-Mattis constraint. When $N = n/\gcd(2, n)$, the system is free from the above constraint and can always be turned into a featureless insulator, as shown by our explicit construction. This implies the possibility of having a direct symmetry mass generation (SMG) transition towards a featurelessly insulator [39].

Our theory will shed light on comprehending the topological nature of correlated semimetals, and in particular their quantum anomaly phenomena. Our results are timely, especially given the rapidly growing list of correlated semimetal candidates, including $\text{Ce}_3\text{Bi}_4\text{Pd}_3$ [40], $\text{Ce}_2\text{Au}_3\text{In}_5$ [41], CaIrO_3 [42], and SrNbO_3 [43], etc. Finally, we highlight that the methodology used in this work is general and directly applicable to other correlated crystalline semimetals. We are thus confident that our framework will pave the way for an unified, beyond-band theory for symmetry-protected semimetallic physics.

ACKNOWLEDGMENTS

S.-J.H. and R.-X.Z. are grateful to the 2018 Boulder Summer School, where this work was initiated. S.-J.H. acknowledges the support from a JQI Postdoctoral Fellowship. J.Y. acknowledges the support by the Gordon and Betty Moore Foundation through the EPiQS Initiative. R.-X.Z. acknowledges the start-up fund of the University of Tennessee. The work done at the University of Maryland is supported by the Laboratory of Physical Sciences.

**APPENDIX A: ZERO MODE SOLUTIONS
OF THE VORTEX-LINE MODES**

To solve the zero mode bound stats at the vortex center, we propose a trial wave function

$$\Psi = [f_1(r)e^{i(J-l-\frac{1}{2})\theta}, f_2(r)e^{i(J-nl_2-l+\frac{1}{2})\theta}], \quad (\text{A1})$$

$$f_3(r)e^{i(J-nl_3+l-\frac{1}{2})\theta}, f_4(r)e^{i(J-nl_4+l+\frac{1}{2})\theta}]^T, \quad (\text{A2})$$

where J is a half-odd integer and $l_2, l_3, l_4 \in \mathbb{Z}$. Plugging into the zero energy equation, we immediately arrive at the following equations:

$$\left[i\partial_r + i\frac{J-nl_2-l+\frac{1}{2}}{r} \right] f_2(r) = mf_3(r)e^{in(l_2-l_3+p)\theta}, \quad (\text{A3})$$

$$\left[i\partial_r - i\frac{J-l-\frac{1}{2}}{r} \right] f_1(r) = mf_4(r)e^{in(p-l_4)\theta}, \quad (\text{A4})$$

$$mf_1(r)e^{in(l_4-p)\theta} = \left[-i\partial_r - i\frac{J-nl_4+l+\frac{1}{2}}{r} \right] f_4(r), \quad (\text{A5})$$

$$mf_2(r)e^{in(l_3-l_2-p)\theta} = \left[-i\partial_r + i\frac{J-nl_3+l-\frac{1}{2}}{r} \right] f_3(r). \quad (\text{A6})$$

It is instructive to integrate out the angular variable θ , and we arrive at

$$\left[i\partial_r + i\frac{J-nl_2-l+\frac{1}{2}}{r} \right] f_2(r) = mf_3(r)\delta_{l_2+p, l_3}, \quad (\text{A7})$$

$$\left[i\partial_r - i\frac{J-l-\frac{1}{2}}{r} \right] f_1(r) = mf_4(r)\delta_{l_4, p}, \quad (\text{A8})$$

$$mf_1(r)\delta_{l_4, p} = \left[-i\partial_r - i\frac{J-nl_4+l+\frac{1}{2}}{r} \right] f_4(r), \quad (\text{A9})$$

$$mf_2(r)\delta_{l_3, l_2+p} = \left[-i\partial_r + i\frac{J-nl_3+l-\frac{1}{2}}{r} \right] f_3(r). \quad (\text{A10})$$

When the delta function in the above equations is evaluated to zero, it is easy to show that we can only have solutions of the form $f_i \sim x^{\alpha_i}$ which are not square integrable. Therefore, the physical solutions are possible only when the following conditions are satisfied:

$$l_3 = l_2 + p, \quad l_4 = p. \quad (\text{A11})$$

In this case we can rewrite our trial wave function as

$$\Psi = [f_1(r)e^{i(J-l-\frac{1}{2})\theta}, f_2(r)e^{i(J'-l+\frac{1}{2})\theta}, f_3(r)e^{i(J'-pn+l-\frac{1}{2})\theta}, f_4(r)e^{i(J'-pn+l+\frac{1}{2})\theta}]^T, \quad (\text{A12})$$

where $J' = J - nl_2$. Then the above equations become

$$\left[i\partial_r + i\frac{J'-l+\frac{1}{2}}{r} \right] f_2(r) = mf_3(r), \quad (\text{A13})$$

$$\left[i\partial_r - i\frac{J-l-\frac{1}{2}}{r} \right] f_1(r) = mf_4(r), \quad (\text{A14})$$

$$mf_1(r) = \left[-i\partial_r - i\frac{J-pn+l+\frac{1}{2}}{r} \right] f_4(r), \quad (\text{A15})$$

$$mf_2(r) = \left[-i\partial_r + i\frac{J'-pn+l-\frac{1}{2}}{r} \right] f_3(r). \quad (\text{A16})$$

Plugging Eq. (A15) into Eq. (A16) and Eq. (A16) into Eq. (A14), we arrive at

$$\left[\partial_\rho^2 + \frac{2l+1-pn}{\rho} \partial_\rho - \frac{\rho^2 + (J+l-pn-\frac{1}{2})(J-l-\frac{1}{2})}{\rho^2} \right] f_1(\rho) = 0, \quad (\text{A17})$$

$$\left[\partial_\rho^2 + \frac{n-2l+p1}{\rho} \partial_\rho - \frac{\rho^2 + (J'+l-pn-\frac{1}{2})(J'-l-\frac{1}{2})}{\rho^2} \right] f_3(\rho) = 0, \quad (\text{A18})$$

where we have defined $\rho = |m|r$. Equations (A17) and (A18) can be unified in a neat form:

$$\left[\partial_\rho^2 + \frac{2\alpha+1}{\rho} \partial_\rho - \frac{\rho^2 + (L-\frac{m+1}{2})^2 - \alpha^2}{\rho^2} \right] f(\rho) = 0, \quad (\text{A19})$$

where

- (1) Eq. (A17): $\alpha = l - \frac{n}{2}$, $L = J$, $f = f_1$,
- (2) Eq. (A18): $\alpha = -(l - \frac{n}{2})$, $L = J'$, $f = f_3$.

It is instructive to define

$$\tilde{f}_\alpha = f\rho^\alpha, \quad (\text{A20})$$

which transforms Eq. (A19) into the modified Bessel equation:

$$\left\{ \rho^2 \partial_\rho^2 + \rho \partial_\rho - \left[\rho^2 + \left(L - \frac{pn+1}{2} \right)^2 \right] \right\} \tilde{f}_\alpha(\rho) = 0. \quad (\text{A21})$$

The decay solution of the above equation is known as the modified Bessel function of the second kind,

$$\tilde{f}_\alpha(\rho) = cK_{L-\frac{pn+1}{2}}(\rho). \quad (\text{A22})$$

Therefore, we arrive at the following solutions for $f_1(\rho)$ and $f_3(\rho)$:

$$f_1(\rho) = c_1 \rho^{\frac{m}{2}-l} K_{J-\frac{m+1}{2}}(\rho),$$

$$f_3(\rho) = c_3 \rho^{-(\frac{m}{2}-l)} K_{J'-\frac{m+1}{2}}(\rho). \quad (\text{A23})$$

Meanwhile, from Eq. (A15) and Eq. (A16), we arrive at

$$f_2(\rho) = ic_3 \rho^{l-\frac{m}{2}} K_{J'-\frac{m-1}{2}}(\rho),$$

$$f_4(\rho) = -ic_1 \rho^{-l+\frac{m}{2}} K_{J-\frac{m-1}{2}}(\rho), \quad (\text{A24})$$

where we have applied the recurrence relation of the modified Bessel functions:

$$\begin{aligned} \left(\partial_x + \frac{n}{x}\right)K_n(x) &= -K_{n-1}(x), \\ \left(\partial_x - \frac{n}{x}\right)K_n(x) &= -K_{n+1}(x). \end{aligned} \quad (\text{A25})$$

In summary, the radial part of the zero mode solutions are

$$\begin{aligned} f_1(\rho) &= c_1 \rho^{\frac{pn}{2}-l} K_{J-\frac{pn+1}{2}}(\rho), \\ f_2(\rho) &= ic_3 \rho^{l-\frac{pn}{2}} K_{J-\frac{pn-1}{2}}(\rho), \\ f_3(\rho) &= c_3 \rho^{l-\frac{pn}{2}} K_{J-\frac{pn+1}{2}}(\rho), \\ f_4(\rho) &= -ic_1 \rho^{\frac{pn}{2}-l} K_{J-\frac{pn-1}{2}}(\rho). \end{aligned} \quad (\text{A26})$$

A physical wave function must be square integrable to be normalizable. The square integrability condition will put a strong constraint on Eq. (A26). Since the modified Bessel function of the second kind is exponentially decaying for large ρ , we need focus only on the small ρ behaviors for the solutions in Eq. (A26). We note that

- If the solution $f(\rho)$ in Eq. (A26) satisfies $|f(\rho)|^2 < \rho^{-2}$ as $\rho \rightarrow 0$, then $f(\rho)$ is square integrable.

By performing the Taylor expansion of $K_n(\rho)$ around $\rho = 0$, we find the dominating contributions are given by

$$\begin{aligned} K_0(\rho) &= -\log \rho + \dots, \\ K_n(\rho) &\sim \rho^{-|n|} + \dots, \quad \forall n \neq 0. \end{aligned} \quad (\text{A27})$$

Thus, it is suggestive to discuss the following situations case by case.

We first solve the case for $\nu = pn - 2l > 0$. When $J = J' = \frac{pn+1}{2}$, we apply the square integrability condition to the zero mode solutions:

- (1) $|f_1(\rho)|^2 \sim \rho^{pn-2l} |K_0(\rho)|^2 = \rho^{pn-2l} (\log \rho)^2 \leq \rho^2 (\log \rho)^2 \rightarrow 0$, as $\rho \rightarrow 0$. Thus, $f_1(\rho)$ is square integrable.
- (2) $|f_2(\rho)|^2 \sim \rho^{2l-pn} |K_1(\rho)|^2 = \rho^{2l-pn-2} \geq \rho^{-4} > \rho^{-2}$, as $\rho \rightarrow 0$. Thus, $f_2(\rho)$ is *not* square integrable.
- (3) $|f_3(\rho)|^2 \sim \rho^{2l-pn} |K_0(\rho)|^2 = \rho^{2l-pn} (\log \rho)^2 \geq \rho^{-2} (\log \rho)^2 > \rho^{-2}$, as $\rho \rightarrow 0$. Thus, $f_3(\rho)$ is *not* square integrable.

- (4) $|f_4(\rho)|^2 \sim \rho^{pn-2l} |K_1(\rho)|^2 = \rho^{pn-2l-2} \rightarrow 0$, as $\rho \rightarrow 0$. Thus, $f_4(\rho)$ is square integrable.

When $J = J' = \frac{pn-1}{2}$, we apply the square integrability condition to the zero mode solutions:

- (1) $|f_1(\rho)|^2 \sim \rho^{pn-2l} |K_{-1}(\rho)|^2 = \rho^{pn-2l-2} \rightarrow 0$, as $\rho \rightarrow 0$. Thus, $f_1(\rho)$ is square integrable.
- (2) $|f_2(\rho)|^2 \sim \rho^{2l-pn} |K_0(\rho)|^2 = \rho^{2l-pn} (\log \rho)^2 \geq \rho^{-2} (\log \rho)^2 > \rho^{-2}$, as $\rho \rightarrow 0$. Thus, $f_2(\rho)$ is *not* square integrable.

- (3) $|f_3(\rho)|^2 \sim \rho^{2l-pn} |K_{-1}(\rho)|^2 = \rho^{2l-pn-2} \geq \rho^{-4} > \rho^{-2}$, as $\rho \rightarrow 0$. Thus, $f_3(\rho)$ is *not* square integrable.

- (4) $|f_4(\rho)|^2 \sim \rho^{pn-2l} |K_0(\rho)|^2 = \rho^{pn-2l} (\log \rho)^2 \leq \rho^2 (\log \rho)^2 \rightarrow 0$, as $\rho \rightarrow 0$. Thus, $f_4(\rho)$ is square integrable.

When $J = J' \neq \frac{pn+1}{2}$ and $J = J' \neq \frac{pn-1}{2}$, we find that

- (1) $|f_1(\rho)|^2 \sim \rho^{pn-2l-|2l-(pn+1)|}$: To make $|f_1(\rho)|^2 < \rho^{-2}$ as $\rho \rightarrow 0$, we require

$$l - \frac{1}{2} < J < pn - l + \frac{3}{2}. \quad (\text{A28})$$

- (2) $|f_2(\rho)|^2 \sim \rho^{2l-pn-|2l-(pn-1)|}$: To make $|f_2(\rho)|^2 < \rho^{-2}$ as $\rho \rightarrow 0$, we require

$$0 \leq \left| J - \frac{(pn-1)}{2} \right| < l - \frac{pn}{2} + 1 \leq 0, \quad (\text{A29})$$

which is impossible.

- (3) $|f_3(\rho)|^2 \sim \rho^{2l-pn-|2l-(pn+1)|}$: To make $|f_3(\rho)|^2 < \rho^{-2}$ as $\rho \rightarrow 0$, we require

$$0 \leq \left| J - \frac{(pn+1)}{2} \right| < l - \frac{pn}{2} + 1 \leq 0, \quad (\text{A30})$$

which is impossible.

- (4) $|f_4(\rho)|^2 \sim \rho^{pn-2l-|2l-(pn-1)|}$: To make $|f_4(\rho)|^2 < \rho^{-2}$ as $\rho \rightarrow 0$, we require

$$l - \frac{3}{2} < J < pn - l + \frac{1}{2}. \quad (\text{A31})$$

Therefore, c_2 and c_3 have to be zero to make the zero mode wave function square integrable. In addition, we would require $l - \frac{1}{2} < J < pn - l + \frac{1}{2}$ to make $f_1(\rho)$ and $f_4(\rho)$ normalizable. To summarize, the zero mode wave function of the Z_n vortex takes the following form:

$$\Psi_{J,p,l}(\rho, \theta) = \frac{\rho^{\frac{pn}{2}-l}}{\sqrt{\mathcal{N}}} \begin{pmatrix} e^{(J-l-\frac{1}{2})\theta} K_{J-\frac{pn+1}{2}}(\rho) \\ 0 \\ 0 \\ -ie^{(J-pn+l+\frac{1}{2})\theta} K_{J-\frac{pn-1}{2}}(\rho) \end{pmatrix}, \quad (\text{A32})$$

where \mathcal{N} is the normalization factor. This solution is physical only when

$$l - \frac{1}{2} < J < pn - l + \frac{1}{2}, \quad (\text{A33})$$

provided that $\nu = pn - 2l > 0$.

Now we solve the case for $\nu = pn - 2l < 0$. When $J = J' = \frac{pn+1}{2}$, we apply the square integrability condition to the zero mode solutions:

- (1) $|f_1(\rho)|^2 \sim \rho^{-|\nu|} |K_0(\rho)|^2 = \rho^{-|\nu|} (\log \rho)^2 \geq \rho^{-2} (\log \rho)^2 > \rho^{-2}$, as $\rho \rightarrow 0$. Thus, $f_1(\rho)$ is *not* square integrable.

- (2) $|f_2(\rho)|^2 \sim \rho^{|\nu|} |K_1(\rho)|^2 = \rho^{|\nu|-2} \leq \rho^0 < \rho^{-2}$, as $\rho \rightarrow 0$. Thus, $f_2(\rho)$ is square integrable.

- (3) $|f_3(\rho)|^2 \sim \rho^{|\nu|} |K_0(\rho)|^2 = \rho^{|\nu|} (\log \rho)^2 \leq \rho^2 (\log \rho)^2 \rightarrow 0$, as $\rho \rightarrow 0$. Thus, $f_3(\rho)$ is square integrable.

- (4) $|f_4(\rho)|^2 \sim \rho^{-|\nu|} |K_1(\rho)|^2 = \rho^{-|\nu|-2} \geq \rho^{-4} > \rho^{-2}$, as $\rho \rightarrow 0$. Thus, $f_4(\rho)$ is *not* square integrable.

When $J = J' = \frac{pn-1}{2}$, we apply the square integrability condition to the zero mode solutions:

- (1) $|f_1(\rho)|^2 \sim \rho^{-|\nu|} |K_{-1}(\rho)|^2 = \rho^{-|\nu|-2} \geq \rho^{-4} > \rho^{-2}$, as $\rho \rightarrow 0$. Thus, $f_1(\rho)$ is *not* square integrable.

- (2) $|f_2(\rho)|^2 \sim \rho^{|\nu|} |K_0(\rho)|^2 = \rho^{|\nu|} (\log \rho)^2 \leq \rho^2 (\log \rho)^2 \rightarrow 0$, as $\rho \rightarrow 0$. Thus, $f_2(\rho)$ is square integrable.

- (3) $|f_3(\rho)|^2 \sim \rho^{|\nu|} |K_{-1}(\rho)|^2 = \rho^{|\nu|-2} \leq \rho^0 < \rho^{-2}$, as $\rho \rightarrow 0$. Thus, $f_3(\rho)$ is square integrable.

- (4) $|f_4(\rho)|^2 \sim \rho^{-|\nu|} |K_0(\rho)|^2 = \rho^{-|\nu|} (\log \rho)^2 \geq \rho^{-2} (\log \rho)^2 > \rho^{-2}$, as $\rho \rightarrow 0$. Thus, $f_4(\rho)$ is *not* square integrable.

When $J = J' \neq \frac{pn+1}{2}$ and $J = J' \neq \frac{pn-1}{2}$, we find that

(1) $|f_1(\rho)|^2 \sim \rho^{-|v|-|2l-(pn+1)|}$: To make $|f_1(\rho)|^2 < \rho^{-2}$ as $\rho \rightarrow 0$, we require

$$0 \leq \left| J - \frac{(pn+1)}{2} \right| < \frac{-|v|}{2} + 1 \leq 0, \quad (\text{A34})$$

which is impossible.

(2) $|f_2(\rho)|^2 \sim \rho^{|v|-|2l-(pn-1)|}$: To make $|f_2(\rho)|^2 < \rho^{-2}$ as $\rho \rightarrow 0$, we require

$$pn - l - \frac{3}{2} < J < l + \frac{1}{2}. \quad (\text{A35})$$

(3) $|f_3(\rho)|^2 \sim \rho^{|v|-|2l-(pn+1)|}$: To make $|f_3(\rho)|^2 < \rho^{-2}$ as $\rho \rightarrow 0$, we require

$$pn - l - \frac{1}{2} < J < l + \frac{3}{2}. \quad (\text{A36})$$

(4) $|f_4(\rho)|^2 \sim \rho^{-|v|-|2l-(pn-1)|}$: To make $|f_4(\rho)|^2 < \rho^{-2}$ as $\rho \rightarrow 0$, we require

$$0 \leq \left| J - \frac{(pn-1)}{2} \right| < \frac{-|v|}{2} + 1 \leq 0, \quad (\text{A37})$$

which is impossible.

Therefore, c_1 and c_4 have to be zero to make the zero mode wave function square integrable. In addition, we would require $pn - l - \frac{1}{2} < J < l + \frac{1}{2}$ to make $f_1(\rho)$ and $f_4(\rho)$ normalizable. To summarize, the zero mode wave function of the Z_n vortex takes the following form:

$$\Psi_{J,p,l}(\rho, \theta) = \frac{\rho^{\frac{m}{2}-l}}{\sqrt{\mathcal{N}}} \begin{pmatrix} 0 \\ e^{i(J-l+\frac{1}{2})\theta} K_{J-\frac{m-1}{2}}(\rho) \\ -ie^{i(J-pm+l-\frac{1}{2})\theta} K_{J-\frac{m+1}{2}}(\rho) \\ 0 \end{pmatrix}, \quad (\text{A38})$$

where \mathcal{N} is the normalization factor. This solution is physical only when

$$pn - l - \frac{1}{2} < J < l + \frac{1}{2}, \quad (\text{A39})$$

provided that $v = pn - 2l < 0$.

APPENDIX B: BOSONIZATION ANALYSIS OF THE 1D VORTEX-LINE MODES

Here we show that a group of vortex-line modes can always be symmetrically gapped out if the net vorticity vanishes. Consider a generic 1D nonchiral theory with the considered relevant symmetries. At the single-particle level, it always has $4\mathcal{N}$ 1d modes at + valley and $4\mathcal{N}$ 1d modes at - valley, where \mathcal{N} is not the same as the number N of 3D Dirac points at one valley since the number of 1D modes also relies on the vortex windings. We can split the $8\mathcal{N}$ modes into \mathcal{N} groups, with each group furnishing irreps of the relevant symmetries. In the following, we focus on one generic group of eight modes.

Given any group of eight modes, we can label the corresponding fermionic fields as

$$(\psi_{1,R}, \psi_{2,R}, \psi_{3,R}, \psi_{4,R}; \psi_{1,L}, \psi_{2,L}, \psi_{3,L}, \psi_{4,L}) \quad (\text{B1})$$

or equivalently, we can define the corresponding boson field vector as

$$\Phi = (\phi_{1,R}, \phi_{2,R}, \phi_{3,R}, \phi_{4,R}; \phi_{1,L}, \phi_{2,L}, \phi_{3,L}, \phi_{4,L})^T. \quad (\text{B2})$$

The Abelian bosonization convention we are following is

$$\psi_L \sim e^{i\phi_L}, \quad \psi_R \sim e^{-i\phi_R}. \quad (\text{B3})$$

Here we have omitted the Klein factors for simplicity. ϕ_L and ϕ_R are the chiral boson fields. The corresponding \mathcal{K} matrix is

$$\mathcal{K} = \begin{pmatrix} \mathbb{I}_4 & 0 \\ 0 & -\mathbb{I}_4 \end{pmatrix}. \quad (\text{B4})$$

The symmetry constraints of Λ_i are listed as follows:

(1) $U(1)_c$: The charge vector \mathbf{t}_c is found to be

$$\mathbf{t}_c = (1, 1, 1, 1; 1, 1, 1, 1)^T \quad (\text{B5})$$

(2) \mathcal{P} :

$$\mathcal{P}\Phi\mathcal{P}^{-1} = \sigma_x \otimes \sigma_0 \otimes \sigma_x \Phi \quad (\text{B6})$$

(3) T_z : Without loss of generality, we assume that the Dirac fermions with the channel index v lives at $k = vk_0$. Then the lattice translation symmetry T_z leads to the valley charge vector \mathbf{t}_v :

$$\mathbf{t}_v = (1, -1, 1, -1; 1, -1, 1, -1)^T \quad (\text{B7})$$

(4) C_n : In the Luttinger liquid language, the C_n symmetry will transform the fermionic modes in the following way:

$$\begin{aligned} C_n \psi_{1,R} C_n^\dagger &= e^{i\frac{2\pi}{n} j_1} \psi_{1,R}, & C_n \psi_{1,L} C_n^\dagger &= e^{i\frac{2\pi}{n} j_2} \psi_{1,L}, \\ C_n \psi_{2,R} C_n^\dagger &= e^{i\frac{2\pi}{n} j_2} \psi_{2,R}, & C_n \psi_{2,L} C_n^\dagger &= e^{i\frac{2\pi}{n} j_1} \psi_{2,L}, \\ C_n \psi_{3,R} C_n^\dagger &= e^{-i\frac{2\pi}{n} j_1} \psi_{3,R}, & C_n \psi_{3,L} C_n^\dagger &= e^{-i\frac{2\pi}{n} j_2} \psi_{3,L}, \\ C_n \psi_{4,R} C_n^\dagger &= e^{-i\frac{2\pi}{n} j_2} \psi_{4,R}, & C_n \psi_{4,L} C_n^\dagger &= e^{-i\frac{2\pi}{n} j_1} \psi_{4,L}. \end{aligned} \quad (\text{B8})$$

Then, in the boson basis,

$$C_n \Phi C_n^\dagger = \Phi - \frac{2\pi}{n} \mathbf{t}_n, \quad (\text{B9})$$

where we have defined

$$\mathbf{t}_n = (j_1, j_2, -j_1, -j_2; j_2, j_1, -j_2, -j_1). \quad (\text{B10})$$

(1) \mathcal{PT} :

$$\mathcal{PT}\Phi\mathcal{PT}^\dagger = -\sigma_0 \otimes \sigma_x \otimes \sigma_0 \Phi + \frac{\pi}{2} \mathbf{t}_{\mathcal{PT}} \quad (\text{B11})$$

with $\mathbf{t}_{\mathcal{PT}} = (1, 1, -1, -1; 1, 1, -1, -1)^T$.

Given the above symmetry transformation of the boson field vector, we find that the gapping vector Λ (which is always real) and its corresponding $\Phi_\Lambda = \Lambda^T \Phi$ must satisfy the following symmetry constraints to preserve required symmetries:

$$U(1)_c : \Lambda^T \mathbf{t}_c = 0,$$

$$T_z : \Lambda^T \mathbf{t}_v = 0,$$

$$C_n : \Lambda^T \mathbf{t}_n = 0 \pmod{2n},$$

$$\mathcal{P} : \cos \Phi_\Lambda = \cos(\Lambda^T \sigma_x \otimes \sigma_0 \otimes \sigma_x \Phi),$$

$$\mathcal{PT} : \cos \Phi_\Lambda = \cos\left(\Lambda^T \sigma_0 \otimes \sigma_x \otimes \sigma_0 \Phi - \frac{\pi}{2} \Lambda^T \mathbf{t}_{\mathcal{PT}}\right). \quad (\text{B12})$$

In addition, Λ needs to be checked to avoid SSB and to satisfy the null vector condition.

Based on the above equation, there are four linearly independent Λ 's that preserve $U(1)_c$, T_z and C_n as

$$\begin{aligned}\Lambda_1 &= (1, 1, 0, 0; -1, -1, 0, 0)^T, \\ \Lambda_2 &= (0, 0, 1, 1; 0, 0, -1, -1)^T, \\ \Lambda_3 &= (1, -1, 0, 0; 0, 0, -1, 1)^T, \\ \Lambda_4 &= (0, 0, 1, -1; -1, 1, 0, 0)^T.\end{aligned}\quad (\text{B13})$$

Furthermore, \mathcal{PT} requires

$$\langle \Phi_{\Lambda_1} \rangle = \langle \Phi_{\Lambda_2} \rangle, \quad \langle \Phi_{\Lambda_3} \rangle = \langle \Phi_{\Lambda_4} \rangle, \quad (\text{B14})$$

whereas the inversion symmetry does not give any extra constraints. Therefore, we have shown the existence of four linearly independent gapping vectors for each group of eight 1D modes.

Next, we show those gapping vectors do not lead to SSB. If the SSB of C_n , \mathcal{P} or \mathcal{PT} symmetry happens, there necessarily exists a nonzero $C_n/\mathcal{P}/\mathcal{PT}$ -breaking order parameter Δ . Generally, Δ is defined as the expectation value of some vortex operator:

$$\Delta = \langle \Omega | e^{i\mathbf{L}_\Delta \cdot \Phi} | \Omega \rangle, \quad (\text{B15})$$

where $|\Omega\rangle$ is any ground state. In fact, $\Delta \neq 0$ is possible if and only if \mathbf{L}_Δ can be linearly expanded in terms of the gapping vectors Λ_i 's:

$$\mathbf{L}_\Delta = \sum_{i=1}^4 c_i \Lambda_i, \quad (\text{B16})$$

where c_i are some coefficients. Otherwise, $e^{i\mathbf{L}_\Delta \cdot \Phi}$ will fluctuate and forces $\Delta = 0$. However, $\Lambda_i^T \mathbf{t}_n = 0$ implies

$$\mathbf{L}_\Delta^T \mathbf{t}_n = 0, \quad (\text{B17})$$

which is independent of our choice of j_1 and j_2 for \mathbf{t}_n . Thus, any nonzero Δ constructed from Λ_i 's must respect C_n symmetry. In other words, all C_n -breaking orders are vanishing in the presence of Λ_i s.

Similarly, the possibility of a \mathcal{P}/\mathcal{PT} -breaking order parameter can be ruled out. By applying the symmetry requirement from Eq. (B14), it is easy to prove

$$\begin{aligned}\langle \mathcal{PT} \Omega | e^{i\mathbf{L}_\Delta \cdot \Phi} | \mathcal{PT} \Omega \rangle &= \Delta, \\ \langle \mathcal{P} \Omega | e^{i\mathbf{L}_\Delta \cdot \Phi} | \mathcal{P} \Omega \rangle &= \Delta,\end{aligned}\quad (\text{B18})$$

when the nonzero condition in Eq. (B16) is satisfied.

Additionally, the Mermin-Wigner theorem ensures that there is no SSB of $U(1)_c$. Since the lattice transition along z , T_z , is equivalent to the valley $U(1)$ at the low energy, the Mermin-Wigner theorem ensures that there is no SSB of T_z . Therefore, we can conclude that Λ_i s do not break any of the relevant symmetries. Thus, each group of eight modes can be gapped out in a symmetry-preserving way, and so is the whole system.

APPENDIX C: REVIEW OF THE CRYSTALLINE GAUGE FIELDS

Here we review the definition of crystalline gauge fields, which was introduced by Thorngren and Else [24] (see also Refs. [24–32]). Recall that a usual gauge field for an internal symmetry is defined as a map $A : M \rightarrow BG$, where BG is the classifying space for a internal symmetry group G . For crystalline symmetry, this definition needs to be generalized since it's usually believed that a crystalline symmetry acts as a combination of internal symmetry and a (subgroup of the) isometry group action on the underlying manifold, and the map A captures only the first part. Thorngren and Else proposed that, when G contains a crystalline symmetry, we should replace the classifying space by a space called the homotopy quotient $X//G$. The space $X//G$ has a concrete construction called a Borel construction (or Borel space), which is defined as $(X \times EG)/G$, where G acts diagonally on the product space $X \times EG$. In practice, we can just define $X//G := (X \times EG)/G$ [44].

Here are some known facts about $X//G$:

- (1) When $G = 1$, $X//G = X$
- (2) When $X = pt$, $X//G \cong BG$
- (3) When $X = \mathbb{R}^d$ (or any contractible space), $X//G \cong BG$
- (4) When G action is free, $X//G \cong X/G$.

Now we review a simplicial complex construction of $X//G$. The 0-simplices of $X//G$ are given by the elements $x \in X$. The 1-simplices $x \rightarrow x'$ are given by the elements $g \in G$ for which $g \cdot x = x'$. A 2-simplex is added for every triple g_1, g_2, g_3 with $g_1 g_2 = g_3$. Higher simplices are also added for all higher relations in the group. A crystalline gauge field is defined as a map $\alpha : M \rightarrow X//G$, where, most of the time, we choose $X = \mathbb{R}^d$. In this case, there is actually a homotopy equivalence: $\mathbb{R}^d//G \cong BG$.

A simple example is given by the discrete translation symmetry $\Gamma \cong \mathbb{Z}$ in one dimension. We choose $X = \mathbb{R}$. Since translation Γ acts freely on \mathbb{R} , the homotopy quotient $X//\Gamma \cong X/\Gamma \cong S^1$.

Let $M = \mathbb{R}$, then there is a G-CW complex decomposition where lattice sites are 0-cells and unit cells are 1-cells. Now consider a dual cell decomposition where the dual 0-cells are located at the center of the unit cell. We can choose the map $t : M \rightarrow \mathbb{R}/\mathbb{Z} \cong S^1$ such that $t(m_n) = x_0$, where $m_n \in M$ is a vertex in the dual cell complex (center of the unit cell) and $x_0 \in \mathbb{R}/\mathbb{Z}^T \cong S^1$ is the based point in S^1 . A dual 1-cell automatically carries a g label, and in this case it's labeled by $1 \in \mathbb{Z}$ since a dual 1-cell is mapped to a 1-simplex $x \rightarrow x'$. We see that the translation gauge field essentially counts the number of sites. We note that the choice of the space $X//G$ is not unique as long as they are homotopy equivalent. In this example, there is a physical choice of the space $X//\Gamma \cong S^1$. We can interpret X as the momentum space, and the homotopy quotient $X//\Gamma \cong S^1$ is precisely the Brillouin zone. The above map t assign a momenta $2\pi n$ to each dual 0-cell labeled by n , where n is an integer, and assign the momentum difference (which must be an integer multiple of the reciprocal lattice vector) between two neighboring unit cells to each dual 1-cell $(n, n+1)$. The translation gauge field t we choose then satisfies the following

property:

$$\int_{P_x} t = 2\pi L, \quad (\text{C1})$$

where P_x is a 1-cycle across the whole system and L is the number of lattice point. The translation gauge field defined in this way is essentially the same as the elasticity tetrad or vielbein [25,26,31,45].

One way to couple a low-energy Dirac theory to a crystalline gauge field is to introduce the spatially dependent mass terms introduced in Ref. [31]. Let \mathcal{P} be the space of parameter of the mass terms, then the crystalline symmetry has a nontrivial actions on P , and generally it's possible to focus on a subspace of P such that the crystalline symmetry acts in the same way as \mathbb{R}^d . We can then formally identify $P \cong X$ and construct the homotopy quotient $P//G$. Therefore, we have a realization of the crystalline gauge field as the map $\alpha : M \rightarrow P//G$, and, specifically, a crystalline gauge field in this representation is given by the pullback of a differential 1-form in the parameter space P .

APPENDIX D: QUANTIZATION CONDITIONS OF CRYSTALLINE GAUGE FIELDS

Here we give more details about the quantization conditions and deformation classes of the translation and rotational gauge fields.

The phase of the mass term $\phi(z)$ lives in the parameter space P with a nontrivial translation symmetry action. As a result, ϕ actually lives in $P//\Gamma_z \cong S^1$, where Γ_z denotes the group of z translation. Therefore, the spatially dependent phase of the mass term in Eq. (7) is a map: $M \rightarrow P//\Gamma_z \cong B\Gamma_z \cong S^1$. The translation gauge field can then be defined explicitly as a differential 1-form $E_z = d\phi/2\pi$, where ϕ is the spatially dependent phase in the mass term (7). We consider the configuration of ϕ such that the translation gauge field satisfies

$$\int_{P_z} E_z = 1, \quad (\text{D1})$$

where P_z is a 1-cycle across one unit cell along the z direction. The translation gauge field, satisfying Eq. (D1), corresponds to the generators in the cohomology group $H^1(B\Gamma, \mathbb{Z}) = \mathbb{Z}$, which counts the number of lattice sites in the z direction [25,26,31,45].

Similarly, the phase of the vortex mass term Eq. (3) gives a map: $M \rightarrow X/C_n \cong BC_n$. We then define the C_n rotational gauge field as a differential 1-form $\omega^{(n)} = dn_\theta/2\pi$, where $n_\theta = \nu\theta$. We consider the configuration of θ such that the rotational gauge field satisfies

$$\int_{P_n} \omega^{(n)} = \frac{\nu}{n} \text{ mod } 1, \quad (\text{D2})$$

where P_n is a 1-cycle with the starting and the points related by the C_n rotation. The rotational gauge field is classified by the cohomology group $H^1(BC_n, \mathbb{Z}) = \mathbb{Z}_n$. The 2-form $d\omega^{(n)}$ constructed by the rotational gauge field in the cohomology class in $H^1(BC_n, \mathbb{Z})$ specified by Eq. (D2) has to satisfy

$$\int_{D_{xy}} d\omega^{(n)} = \nu \text{ mod } n, \quad (\text{D3})$$

where D_{xy} is any two-dimensional (2D) disk containing the rotational axis along the xy direction. This can be seen by the Stokes theorem:

$$\int_{D_{xy}} d\omega^{(n)} = \int_{\partial D_{xy}} \omega^{(n)} \quad (\text{D4})$$

$$= n \int_{P_n} d\omega^{(n)} \quad (\text{D5})$$

$$= \nu \text{ mod } n, \quad (\text{D6})$$

where in the second equality we have used the fact that any 2D disk can be deformed into a disk respecting the C_n rotation and the boundary of such disk is the union of the 1-cycle P_n .

APPENDIX E: CLASSIFICATION DETAILS IN THE TOPOLOGICAL FIELD THEORY

We now solve

$$N\nu \text{ mod } n = 0 \text{ and } N \in \mathbb{Z} \quad (\text{E1})$$

for N under the assumption that

$$\nu \in \mathbb{Z} - \{0\}, \quad n \in \{1, 2, 3, \dots\}. \quad (\text{E2})$$

First, we note that Eq. (E1) is equivalent to

$$N|\nu| \in n\mathbb{Z} \text{ and } N|\nu| \in |\nu|\mathbb{Z}, \quad (\text{E3})$$

which is further equivalent to

$$N|\nu| \in |\nu|\mathbb{Z} \cap n\mathbb{Z}. \quad (\text{E4})$$

Therefore, the solution set to Eq. (E1) is

$$\frac{|\nu|\mathbb{Z} \cap n\mathbb{Z}}{|\nu|}. \quad (\text{E5})$$

Note that $|\nu|\mathbb{Z} \cap n\mathbb{Z}$ is the set of all common multiples of $|\nu|$ and n , which is further equal to the set of multiples of $\text{lcm}(|\nu|, n)$, where $\text{lcm}(|\nu|, n)$ is the least common multiple of $|\nu|$ and n [46]. It means that we have

$$|\nu|\mathbb{Z} \cap n\mathbb{Z} = \text{lcm}(|\nu|, n)\mathbb{Z}. \quad (\text{E6})$$

Owing to $\text{lcm}(|\nu|, n) \text{gcd}(|\nu|, n) = |\nu|n$ [46], the solution set to Eq. (E1) eventually becomes

$$\begin{aligned} \frac{|\nu|\mathbb{Z} \cap n\mathbb{Z}}{|\nu|} &= \frac{\text{lcm}(|\nu|, n)\mathbb{Z}}{|\nu|} = \frac{|\nu|n}{\text{gcd}(|\nu|, n)|\nu|}\mathbb{Z} \\ &= \frac{n}{\text{gcd}(|\nu|, n)}\mathbb{Z}. \end{aligned} \quad (\text{E7})$$

[1] A. A. Burkov, Topological semimetals, *Nat. Mater.* **15**, 1145 (2016).

[2] B. Yan and C. Felser, Topological materials: Weyl semimetals, *Annu. Rev. Condens. Matter Phys.* **8**, 337 (2017).

- [3] A. Bernevig, H. Weng, Z. Fang, and X. Dai, Recent progress in the study of topological semimetals, *J. Phys. Soc. Jpn.* **87**, 041001 (2018).
- [4] N. P. Armitage, E. J. Mele, and A. Vishwanath, Weyl and Dirac semimetals in three-dimensional solids, *Rev. Mod. Phys.* **90**, 015001 (2018).
- [5] S. M. Young, S. Zaheer, J. C. Y. Teo, C. L. Kane, E. J. Mele, and A. M. Rappe, Dirac semimetal in three dimensions, *Phys. Rev. Lett.* **108**, 140405 (2012).
- [6] Z. Wang, Y. Sun, X.-Q. Chen, C. Franchini, G. Xu, H. Weng, X. Dai, and Z. Fang, Dirac semimetal and topological phase transitions in $A_3\text{Bi}$ ($A = \text{Na, K, Rb}$), *Phys. Rev. B* **85**, 195320 (2012).
- [7] Z. Wang, H. Weng, Q. Wu, X. Dai, and Z. Fang, Three-dimensional Dirac semimetal and quantum transport in Cd_3As_2 , *Phys. Rev. B* **88**, 125427 (2013).
- [8] Z. K. Liu, B. Zhou, Y. Zhang, Z. J. Wang, H. M. Weng, D. Prabhakaran, S.-K. Mo, Z. X. Shen, Z. Fang, X. Dai *et al.*, Discovery of a three-dimensional topological Dirac semimetal, Na_3Bi , *Science* **343**, 864 (2014).
- [9] M. Neupane, S.-Y. Xu, R. Sankar, N. Alidoust, G. Bian, C. Liu, I. Belopolski, T.-R. Chang, H.-T. Jeng, H. Lin *et al.*, Observation of a three-dimensional topological Dirac semimetal phase in high-mobility Cd_3As_2 , *Nat. Commun.* **5**, 3786 (2014).
- [10] B.-J. Yang and N. Nagaosa, Classification of stable three-dimensional Dirac semimetals with nontrivial topology, *Nat. Commun.* **5**, 4898 (2014).
- [11] B.-J. Yang, T. Morimoto, and A. Furusaki, Topological charges of three-dimensional Dirac semimetals with rotation symmetry, *Phys. Rev. B* **92**, 165120 (2015).
- [12] R.-X. Zhang, Y.-T. Hsu, and S. Das Sarma, Higher-order topological Dirac superconductors, *Phys. Rev. B* **102**, 094503 (2020).
- [13] L. Fidkowski and A. Kitaev, Effects of interactions on the topological classification of free fermion systems, *Phys. Rev. B* **81**, 134509 (2010).
- [14] H. Yao and S. Ryu, Interaction effect on topological classification of superconductors in two dimensions, *Phys. Rev. B* **88**, 064507 (2013).
- [15] H. Isobe and L. Fu, Theory of interacting topological crystalline insulators, *Phys. Rev. B* **92**, 081304(R) (2015).
- [16] H. Song, S.-J. Huang, L. Fu, and M. Hermele, Topological phases protected by point group symmetry, *Phys. Rev. X* **7**, 011020 (2017).
- [17] X.-Y. Song and A. P. Schnyder, Interaction effects on the classification of crystalline topological insulators and superconductors, *Phys. Rev. B* **95**, 195108 (2017).
- [18] Ö. M. Aksoy, J.-H. Chen, S. Ryu, A. Furusaki, and C. Mudry, Stability against contact interactions of a topological superconductor in two-dimensional space protected by time-reversal and reflection symmetries, *Phys. Rev. B* **103**, 205121 (2021).
- [19] S.-J. Huang, H. Song, Y.-P. Huang, and M. Hermele, Building crystalline topological phases from lower-dimensional states, *Phys. Rev. B* **96**, 205106 (2017).
- [20] K. Shiozaki, C. Z. Xiong, and K. Gomi, Generalized homology and Atiyah-Hirzebruch spectral sequence in crystalline symmetry protected topological phenomena, *Prog. Theor. Exp. Phys.* **2023**, 083101 (2023).
- [21] Z. Song, S.-J. Huang, Y. Qi, C. Fang, and M. Hermele, Topological states from topological crystals, *Sci. Adv.* **5**, eaax2007 (2019).
- [22] D. V. Else and R. Thorngren, Crystalline topological phases as defect networks, *Phys. Rev. B* **99**, 115116 (2019).
- [23] Z. Song, C. Fang, and Y. Qi, Real-space recipes for general topological crystalline states, *Nat. Commun.* **11**, 4197 (2020).
- [24] R. Thorngren and D. V. Else, Gauging spatial symmetries and the classification of topological crystalline phases, *Phys. Rev. X* **8**, 011040 (2018).
- [25] J. Nissinen and G. E. Volovik, Tetrads in solids: From elasticity theory to topological quantum Hall systems and Weyl fermions, *J. Exp. Theor. Phys.* **127**, 948 (2018).
- [26] J. Nissinen, Field theory of higher-order topological crystalline response, generalized global symmetries and elasticity tetrads, *Annals Phys.* **447**, 169139 (2022).
- [27] X.-Y. Song, Y.-C. He, A. Vishwanath, and C. Wang, Electric polarization as a nonquantized topological response and boundary Luttinger theorem, *Phys. Rev. Res.* **3**, 023011 (2021).
- [28] L. Gioia, C. Wang, and A. A. Burkov, Unquantized anomalies in topological semimetals, *Phys. Rev. Res.* **3**, 043067 (2021).
- [29] N. Manjunath and M. Barkeshli, Crystalline gauge fields and quantized discrete geometric response for Abelian topological phases with lattice symmetry, *Phys. Rev. Res.* **3**, 013040 (2021).
- [30] J. May-Mann and T. L. Hughes, Crystalline responses for rotation-invariant higher-order topological insulators, *Phys. Rev. B* **106**, L241113 (2022).
- [31] S.-J. Huang, C.-T. Hsieh, and J. Yu, Effective field theories of topological crystalline insulators and topological crystals, *Phys. Rev. B* **105**, 045112 (2022).
- [32] J. May-Mann, M. R. Hirsbrunner, X. Cao, and T. L. Hughes, Topological field theories of three-dimensional rotation symmetric insulators: Coupling curvature and electromagnetism, *Phys. Rev. B* **107**, 205149 (2023).
- [33] Most existing DSM materials, such as Na_3Bi and Cd_3As_2 , belong to this representation of inversion operator. The other possible choice is $\mathcal{P} \doteq s_x \otimes \gamma_0$. These choices won't affect the classification.
- [34] R.-X. Zhang, J. A. Hutasoit, Y. Sun, B. Yan, C. Xu, and C.-X. Liu, Topological nematic phase in Dirac semimetals, *Phys. Rev. B* **93**, 041108(R) (2016).
- [35] A. M. Turner, E. Berg, and A. Stern, Gapping fragile topological bands by interactions, *Phys. Rev. Lett.* **128**, 056801 (2022).
- [36] We note that these classification is valid when κ (hence the momentum separation of the Dirac points) doesn't belong to the set of exceptional values: $\kappa_{ex} = p/(v + qn)$, where p and q are integers. When $\kappa = \kappa_{ex}$, we can shift the rational gauge field $\omega^{(n)}$ by a coboundary such that $\int d\omega^{(n)} = v + qn$, and the anomaly is in fact trivial. This implies that the Dirac points can be gapped out symmetrically by strong interactions. Note that shifting the quantization condition of $d\omega^{(n)}$ might require introducing additional bands in practice. Similar conclusions of the exceptional values are obtained in Ref. [28] for different topological semimetals.
- [37] S. Raza, A. Sirota, and J. C. Y. Teo, From Dirac semimetals to topological phases in three dimensions: A coupled-wire construction, *Phys. Rev. X* **9**, 011039 (2019).

- [38] C. Wang, L. Gioia, and A. A. Burkov, Fractional quantum Hall effect in Weyl semimetals, *Phys. Rev. Lett.* **124**, 096603 (2020).
- [39] J. Wang and Y.-Z. You, Symmetric mass generation, *Symmetry* **14**, 1475 (2022).
- [40] S. Dzsaber, L. Prochaska, A. Sidorenko, G. Eguchi, R. Svagera, M. Waas, A. Prokofiev, Q. Si, and S. Paschen, Kondo insulator to semimetal transformation tuned by spin-orbit coupling, *Phys. Rev. Lett.* **118**, 246601 (2017).
- [41] L. Chen, C. Setty, H. Hu, M. G. Vergniory, S. E. Grefe, L. Fischer, X. Yan, G. Eguchi, A. Prokofiev, S. Paschen *et al.*, Topological semimetal driven by strong correlations and crystalline symmetry, *Nat. Phys.*, **18**, 1341 (2022).
- [42] J. Fujioka, R. Yamada, M. Kawamura, S. Sakai, M. Hirayama, R. Arita, T. Okawa, D. Hashizume, M. Hoshino, and Y. Tokura, Strong-correlation induced high-mobility electrons in Dirac semimetal of perovskite oxide, *Nat. Commun.* **10**, 362 (2019).
- [43] J. M. Ok, N. Mohanta, J. Zhang, S. Yoon, S. Okamoto, E. S. Choi, H. Zhou, M. Briggeman, P. Irvin, A. R. Lupini *et al.*, Correlated oxide Dirac semimetal in the extreme quantum limit, *Sci. Adv.* **7**, eabf9631 (2021).
- [44] It's called a homotopy quotient because it behaves nicely under homotopy. Given two G spaces X, Y and a homotopy equivalence $f : X \rightarrow Y$ with f being equivariant, the induced map $X//G \rightarrow Y//G$ will be a homotopy equivalence.
- [45] D. V. Else, S.-J. Huang, A. Prem, and A. Gromov, Quantum many-body topology of quasicrystals, *Phys. Rev. X* **11**, 041051 (2021).
- [46] P. B. Garrett, *Abstract Algebra* (CRC Press, Boca Raton, FL, 2007).